Sustained Drug Release in Nanomedicine: A Long-Acting Nanocarrier-Based Formulation for Glaucoma

Jayaganesh V. Natarajan,[†] Anastasia Darwitan,[†] Veluchamy A. Barathi,[‡] Marcus Ang,[§] Hla Myint Htoon,[‡] Freddy Boey,[†] Kam C. Tam,[⊥] Tina T. Wong,[†,‡,§,*] and Subbu S. Venkatraman[†,*]

[†]School of Materials Science and Engineering, Nanyang Technological University, Blk N4.1, Nanyang Avenue, Singapore 639798, [‡]Singapore Eye Research Institute, c/o Singapore National Eye Centre, 11 Third Hospital Avenue, Singapore 168751, [§]Singapore National Eye Centre, 11 Third Hospital Avenue, Singapore 168751, and [⊥]Chemical Engineering, University of Waterloo, 200 University Avenue West, Waterloo, Ontario, N2L 3G1, Canada

ABSTRACT Therapeutic nanomedicine has concentrated mostly on anticancer therapy by making use of the nanosize for targeted therapy. Such nanocarriers are not expected to have sustained release of the bioactive molecule beyond a few days. There are other conditions where patients can benefit from sustained duration of action following a single instillation, but achieving this has been difficult in nanosized carriers. An important prerequisite for sustained delivery over several months is to have sufficiently high drug loading, without disruption or changes to the shape of the nanocarriers. Here we report on successful development of a drug-encapsulated nanocarrier for reducing intraocular pressure in a diseased nonhuman primate model and explain why it has been possible to achieve sustained action *in vivo*. The drug is a prostaglandin derivative, latanoprost, while the carrier is a nanosized unilamellar vesicle. The mechanistic details of this unique drug–nanocarrier combination were elucidated by isothermal titration calorimetry. We show, using Cryo-TEM and dynamic light scattering, that the spherical shape of the liposomes is conserved even at the highest loading of latanoprost and that specific molecular interactions between the drug and the lipid are the reasons behind improved stability and sustained release. The *in vivo* results clearly attest to sustained efficacy of lowering the intraocular pressure for 120 days, making this an excellent candidate to be the first truly sustained-release nanomedicine product. The mechanistic details we have uncovered should enable development of similar systems for other conditions where sustained release from nanocarriers is desired.

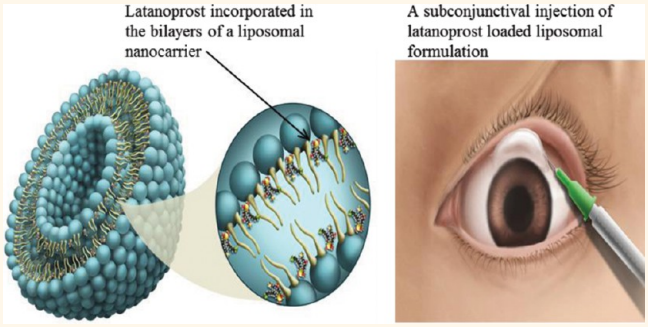

KEYWORDS: sustained drug delivery · nanocarrier · drug–liposomal interactions · nanomedicine · glaucoma

Nanotechnology refers to the engineering of materials at the atomic scale comprising molecular structures in the size range 1–100 nm in at least one dimension.[1] One of the emerging applications of nanotechnology is "nanomedicine".[2] Nanomedicine is a term used to describe the use of nanotechnology to solve medical problems.[3] By far, the major thrust of using nanoparticles for drug or gene delivery has been to enhance cellular penetration[2,4] and not for sustained release. Surprisingly, it has been much more difficult to use nanotechnology to develop viable sustained-release products, in spite of the widely recognized need for such methods to improve management of chronic diseases that require long-term medication. A number of nanoparticles have been evaluated over the years to improve loading and sustained delivery of drugs, including liposomes[5] and polymer nanoparticles.[6,7] Among the nanoparticles studied, liposomes have been the most successful drug delivery carriers.[5] The first successful nanocarrier for drug delivery was Doxil, which used nanosized liposomes that had a "corona" of polyethylene glycol molecules.[8]

Since the introduction of Doxil, several other liposomal products have been developed and approved for human use

* Address correspondence to assubbu@ntu.edu.sg; tina.wong.t.l@snec.com.sg.

Received for review September 3, 2013 and accepted December 31, 2013.

Published online January 06, 2014
10.1021/nn4046024

(Supplementary Table S1).[9] According to a 2006 article, only 38 products have been commercialized in the nanomedicine area, with 23 of these being classified as drug delivery products; of these 23 products, there are only three that can possibly lay claim to be sustained-release (~5 days of release) products.[3] In general, as most of these products were meant for intravenous administration, there was no compelling need for sustained release longer than the half-life of the injected carriers in the blood. If sustained release can be achieved in nanoliposomes, along with enhanced stability of storage of liposomal suspensions, then the scope of disease targets broadens. A good example is the medical treatment of glaucoma. Glaucoma is a progressive optic neuropathy that causes irreversible blindness and affects over 60 million worldwide.[10] Elevated intraocular pressure (IOP) is the main modifiable risk factor. Currently, use of daily eye drops to lower the IOP is the chosen route of drug administration to the patient.[11] The drug bioavailability is only 5% at best,[12] and duration of action is limited to 24 h. Patient compliance is a major challenge and sporadic,[13,14] and if not sustained long-term, leads to disease progression and irreversible blindness. There is an immediate need for a sustained-delivery product for glaucoma medical therapy.

Sufficiently high loading of drug is a necessary prerequisite to sustained delivery over months. Thus, the challenge is to load high concentrations of lipophilic drugs into liposomal nanocarriers without disruption/changes to vesicle shape and to sustain their release over time. Previously, our group reported on the development of a liposomal nanocarrier (average size ~100 nm) loaded with a lipophilic drug, latanoprost, for treatment of glaucoma.[15] In this paper, we report on the sustained efficacy of action of this nanomedicine product in a diseased nonhuman primate model, as well as on mechanistic details of the stability and sustained release obtainable with this drug–nanocarrier combination. In particular, we ask the following questions:

1. Is this drug–liposome combination a very specific one, or can they be applied more generally to other nanocarrier and drug types?
2. Why is this liposomal formulation stable against aggregation, and how is the sustained release achieved?
3. Does the sustained *in vitro* release translate into sustained efficacy of action *in vivo*?

In addition to the *in vitro* results, we also report on the results of a subconjunctival injection of this formulation in a diseased nonhuman primate model. The results clearly attest to sustained efficacy of lowering the intraocular pressure for 120 days and make this an excellent candidate to be the first truly sustained-release nanomedicine product.

RESULTS AND DISCUSSION

Drug Loading and *in Vitro* Release. The first nanocarrier product to be approved by the U.S. FDA was Doxil in 1995. The key to its success as a chemotherapeutic were twofold: first the liposomal doxorubicin had a long blood circulation time (~45–60 h); second, the drug loading in the core of the liposome was high enough (~12.5%) for therapeutic efficacy.[16] None of the other approved liposomal nanomedicine products have any claim to sustained release exceeding 5 days, mostly because the applications considered do not demand sustained release. Conversely, the difficulty in controlling sustained release of drugs from a liposomal nanocarrier may have prevented its broader application. In fact we believe this to be true, from our own attempts to prolong release beyond one week; there are indeed very few reports of sustained release from nanosized liposomes.[17,18]

Why is it difficult to control drug release from nanoliposomes? We believe there are a number of reasons for this. First, if a hydrophilic drug is loaded into the core and the bilayer acts as a membrane to control diffusional release, then the "rigidity" of the membrane is the only factor that can be used to control the diffusion (as the bilayer thickness is on the order of 5–7 nm). Researchers have attempted to do this by adding cholesterol to the bilayer[19,20] or by selecting lipid structures that have a high transition temperature.[18,21] However, using this approach, the slowest release that has been achieved to date is about 8–12 h *in vitro* for doxorubicin.[22] Second, when drug is loaded into the bilayer, the stability of the self-assembled vesicle is severely compromised at a moderate drug loading level (drug to lipid ratios of 0.05 or above); consequently, release rates have been reported to be sustained over only a few days for a number of hydrophobic drugs[23,24] with the exception of one study that showed sustained release over four weeks,[25] using a very lipophilic compound in a mixture of liposomes. In summary, we believe that the difficulty of attaining sustained periods of release from nanoliposomes is primarily due to the lack of diffusion control, due to the very short diffusion path lengths (~5 to 10 nm, the thickness of the bilayer).

We have designed a nanoliposomal–drug combination that can sustain the release of latanoprost beyond 30 days (60% of the cumulative drug is released in 30 days, with subsequent slower release), as seen in an *in vitro* experiment (Supplementary Figure S1). Our approach was based on controlling the release through partitioning rather than through diffusion. This approach allows for higher loading (~1 mg/mL, drug/lipid (D/L) wt ratio of 0.1) as well as for slower release. Although similarly high D/L mole ratios have been reported for other lipophilic drugs such as curcumin (0.07),[26] an aryl-imidazole compound

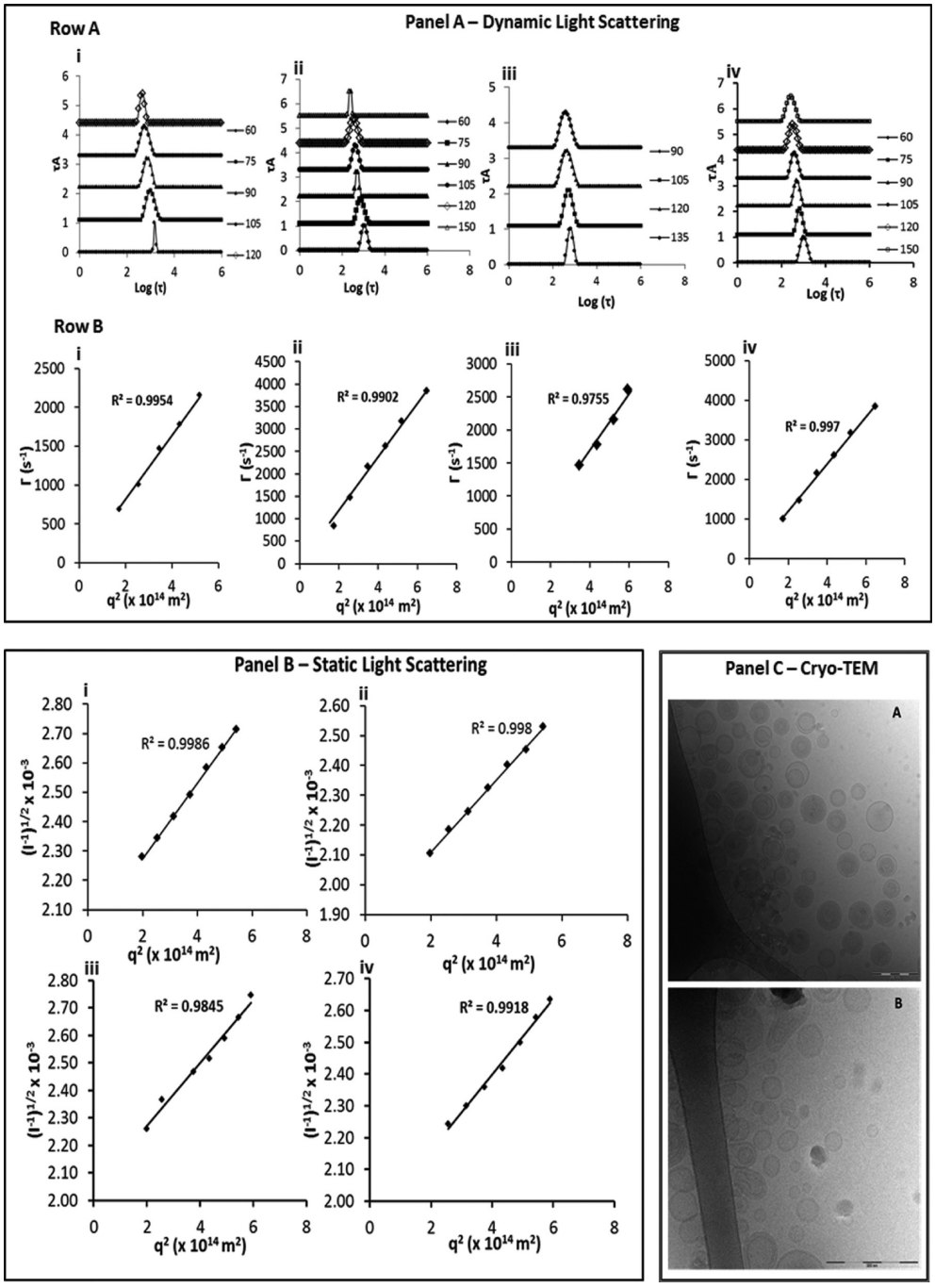

Figure 1. Panel A: Dynamic light scattering measurements: (Row A) Relaxation time distribution functions of liposomes measured at different scattering angles. (i), (ii), (iii), and (iv) represent plain EggPC liposomes at 25 °C, plain EggPC liposomes at 37 °C, latanoprost-loaded EggPC liposomes at 25 °C, and latanoprost-loaded EggPC liposomes at 37 °C . (Row B) Decay rate dependence (Γ) *vs* square of the scattering vector (q^2). (i), (ii), (iii), and (iv) represent plain EggPC liposomes at 25 °C, plain EggPC liposomes at 37 °C, latanoprost-loaded EggPC liposomes at 25 °C, and latanoprost-loaded EggPC liposomes at 37 °C. Panel B: Static light scattering measurements: Debye plot of square root of inverse intensity of scattered light *vs* square of the scattering vector for a single known concentration of liposomes (0.09 mM) with varying angles (55−135°). (i), (ii), (iii), and (iv) represent plain EggPC liposomes at 25 °C, plain EggPC liposomes at 37 °C, latanoprost-loaded EggPC liposomes at 25 °C, and latanoprost-loaded EggPC liposomes at 37 °C. Panel C: Cryo-TEM images: (A) Plain EggPC liposomes after extrusion. Scale bar: 200 nm. Magnification: 25 000×. (B) Latanoprost-loaded EggPC liposomes after extrusion. The liposomes are predominantly spherically shaped with few deformed liposomes. No significant aggregation of liposomes was observed. Scale bar: 200 nm. Magnification: 50 000×.

(ML220, 0.29),[25] and paclitaxel (0.15),[27] the release of these drugs from nanocarriers remains limited to a few weeks. Loading of hydrophobic drugs is often a challenge that is associated with the destabilization of bilayers with increase in drug concentrations.[28,29] Such instability in size precludes the use of nanocarriers for sustained release. In our previous paper, we have shown that the size of our liposomal nanocarriers

TABLE 1. Summary of Hydrodynamic Radius (R_h), Radius of Gyration (R_g), Translational Diffusion Coefficient (D_t), and Shape Factor (S) for Plain EggPC and Latanoprost-Loaded EggPC Liposomes at 25 and 37 °C

	temperature (25 °C)				temperature (37 °C)			
	DLS	SLS	D_t	shape factor	DLS	SLS	D_t	shape factor
type of liposome	R_h (nm)	R_g (nm)	($\times 10^{-12}$ m^2/s)	R_g/R_h	R_h (nm)	R_g (nm)	($\times 10^{-12}$ m^2/s)	R_g/R_h
plain EggPC liposomes	59.7	61.8	4	1.03	54.4	62.4	6	1.15
latanoprost loaded EggPC liposomes	57.8	58.2	4	1.01	54.2	54.8	6	1.01

remained fairly unchanged on storage, suggesting that latanoprost incorporation does not destabilize the bilayer.[15] In this paper, we report more detailed studies on the size and shape changes, as these are key factors to its use as an injectable formulation with predictable performance *in vivo,* as well as for long-term storage without lyophilization.

Size and Shape Changes of Drug-Loaded Nanocarriers. To assess the size and shape, multiangle dynamic and static light scattering were used to determine hydrodynamic radius (R_h) and radius of gyration (R_g), respectively. Figure 1 panel A shows the relaxation time distribution obtained from dynamic light scattering. It is evident (Figure 1, row A) that the relaxation time distribution function is unimodal at all scattering angles and that it shifts to lower relaxation time with increasing scattering angles for both plain and latanoprost-loaded liposomes at both 25 and 37 °C. When the decay rate Γ was plotted against the square of the scattering vector q^2 in Figure 1 (row B), a linear relationship with q^2 was obtained for all the liposomes evaluated (R^2 value of at least 0.98, with the slope of the decay rate Γ *vs* q^2 yielding a value for the translational diffusion coeffcieint (D_t)). The apparent R_h was then calculated from the Stokes–Einstein equation. The estimated values for R_h and D_t for all the liposomes evaluated are summarized in Table 1, where the average (R_h) of plain and latanoprost-loaded liposomes falls within the range 54–60 nm at 25 and 37 °C. An important observation was that R_h variations were minimal with latanoprost loading and temperature. The values of D_t of liposomes were higher at 37 °C than at 25 °C (Table 1), suggesting that liposomes undergo Brownian motion with an apparent increase in D_t with increasing temperature.

In striking similarity to the observations on R_h, the R_g values also exhibit nonvariance with latanoprost addition. The values of R_g estimated (using the partial Berry plot, from the slope of the square root of the inverse intensity of scattered light *vs* q^2) are summarized in Table 1, with most values falling in the range 54–63 nm. There were minimal differences in the R_g values between plain (62 nm) and latanoprost-loaded egg phosphatidylcholine (EggPC) liposomes (58 nm) at 25 °C (Table 1). It is evident that R_g values remain unchanged with latanoprost incorporation; thus there is no evidence of aggregation or an increase in particle size with latanoprost incorporation.

The magnitude of the shape factor (R_g/R_h) is used to determine the morphology of a carrier system. From Table 1, it is seen that the shape factor for both plain and drug-loaded liposomes was approximately unity, which is consistent with a spherical morphology for the vesicles. This result confirms that the shape of the spherical liposomes was conserved even at the highest loading concentration of latanoprost into EggPC liposomes; the self-assembled vesicle morphology was retained at both 25 and 37 °C.

The spherical shape retention with high drug loading was also directly confirmed by Cryo-TEM. The morphological features (size and shape) of plain and drug-loaded liposomes are shown in Figure 1, panel C. As seen in Figure 1 panel C-A, the majority of EggPC liposomes have an average size around 100 nm. Populations of uni-, bi-, and multilamellar liposomes do seem to coexist and were observed to be spherically shaped. In Figure 1 panel C-B, latanoprost-loaded liposomes were predominantly spherically shaped with a few deformed liposomes having a mean size of about 100 nm. The majority of population of vesicles was observed to be unilamellar. There was no significant aggregation of drug-loaded liposomes observed even at this high drug loading.

Drug–Liposomal Interactions by Isothermal Titration Calorimetry. The ratio of the drug concentration in the lipid phase to that in the continuous phase determines the partition coefficient. From our previous studies, we found that more than 95% of the drug was associated with the lipid bilayer, suggesting favorable association of the drug with fluid bilayers of EggPC.[15] We believe that the high loading we achieved in the bilayer without disrupting liposomal self-assemblies and the sustained release over 30 days *in vitro* are both related to favorable drug–lipid interactions and perhaps to a lesser extent by steric factors. To better understand the nature and extent of these interactions, we undertook isothermal titration calorimetric (ITC) studies. The main advantage of using an ITC instrument is that in a single experiment, different thermodynamic parameters such as enthalpy (ΔH), entropy ($T\Delta S$), and free energy (ΔG) of drug–lipid

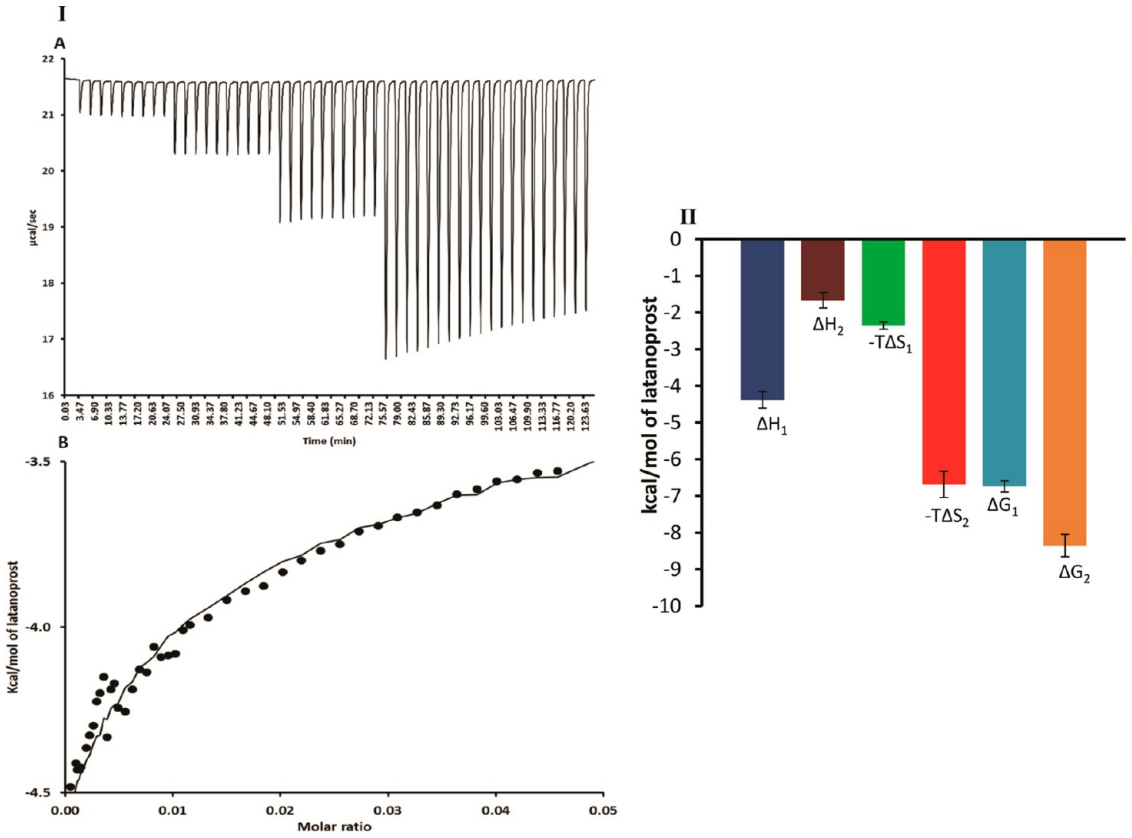

Figure 2. I: (A) Thermogram showing heat rates of latanoprost (μcal/s) *vs* time obtained by titration of latanoprost (2.54 mM) into EggPC liposomes (10.8 mM) with matching solvent mixture (40% DMSO/60% PBS pH 5.5) at 37 °C. Refer to Supplementary Figure S3 for batch 2 and batch 3 thermograms showing heat rates of latanoprost (μcal/s) *vs* time. (B) Enthalpy (kcal/mol of latanoprost) *vs* molar ratio binding curve after background subtraction (heat of dilution from PBS pH 5.5 titrated into the same solvent mixture 40% DMSO/60% PBS pH 5.5 at 37 °C). (Refer to Supplementary Figure S3 for batch 2 and batch 3 for enthalpy (kcal/mol of latanoprost) *vs* molar ratio binding curve after background subtraction). II: Thermodynamic signatures. Latanoprost interactions with EggPC liposomes at binding sites 1 and 2 determined at 37 °C. The parameters such as enthalpy (ΔH_1, ΔH_2), entropy ($T\Delta S_1$, $T\Delta S_2$), and Gibb's free energy (ΔG_1, ΔG_2) are reported based on mean values of three batches, and standard deviations are reported in error bars. Hydrogen bonding and weak van der Waals interactions contribute to favorable enthalpy, while desolvation of both polar and nonpolar groups contributes to favorable entropy. The binding affinity of a drug to its target is dictated by Gibbs' free energy ($\Delta G = \Delta H - T\Delta S$), which is determined by both enthalpy and entropy.

TABLE 2. Summary of Average Latanoprost Binding Affinity (K_1, K_2), Average Enthalpy (ΔH_1, ΔH_2), Average Entropy ($T\Delta S_1$, $T\Delta S_2$), and Average Gibbs Free Energy (ΔG_1, ΔG_2) at Binding Sites 1 and 2 in EggPC Liposomes Measured at 37 °C by Isothermal Titration Calorimetry

thermodynamic parameters	average values ± standard deviation (n = 3)
K_1 ($\times 10^5$ M^{-1})	0.57 ± 0.13
K_2 ($\times 10^5$ M^{-1})	8.42 ± 4.06
ΔH_1 (kcal/mol)	−4.38 ± 0.22
ΔH_2 (kcal/mol)	−1.67 ± 0.21
$T\Delta S_1$ (kcal/mol)	2.36 ± 0.10
$T\Delta S_2$ (kcal/mol)	6.69 ± 0.36
ΔG_1 (kcal/mol)	−6.74 ± 0.15
ΔG_2 (kcal/mol)	−8.35 ± 0.31

binding as well as the binding affinity (K_a) can be evaluated.[30]

Figure 2I A shows the raw data for the heat rates of latanoprost (μcal/s) *vs* time obtained by titrating latanoprost into EggPC liposomes. As seen from the thermogram, the latanoprost binding with EggPC liposome was exothermic. Figure 2I B shows the enthalpy (kcal/mol of latanoprost) *vs* molar ratio binding curve after background subtraction for EggPC liposomes at 37 °C (refer to Supplementary Figure S3 for batch 2 and batch 3). The curve was best fitted with a sequential binding model, with two sites available for latanoprost binding with EggPC liposomes. Thermodynamic signatures of latanoprost interactions with EggPC liposomes at binding sites 1 and 2 estimated at 37 °C are shown in Figure 2II, and their values are summarized in Table 2. The binding affinity (K_a) of the drug to its target is governed by Gibbs free energy ($\Delta G = -RT \ln K_a$). A sufficiently large and negative ΔG leads to a high binding affinity of the drug to its target. The binding affinities of latanoprost were found to be in the micromolar range (Table 2), suggesting that latanoprost interactions with liposomes were highly favorable. To learn more about the precise nature of these interactions, it is

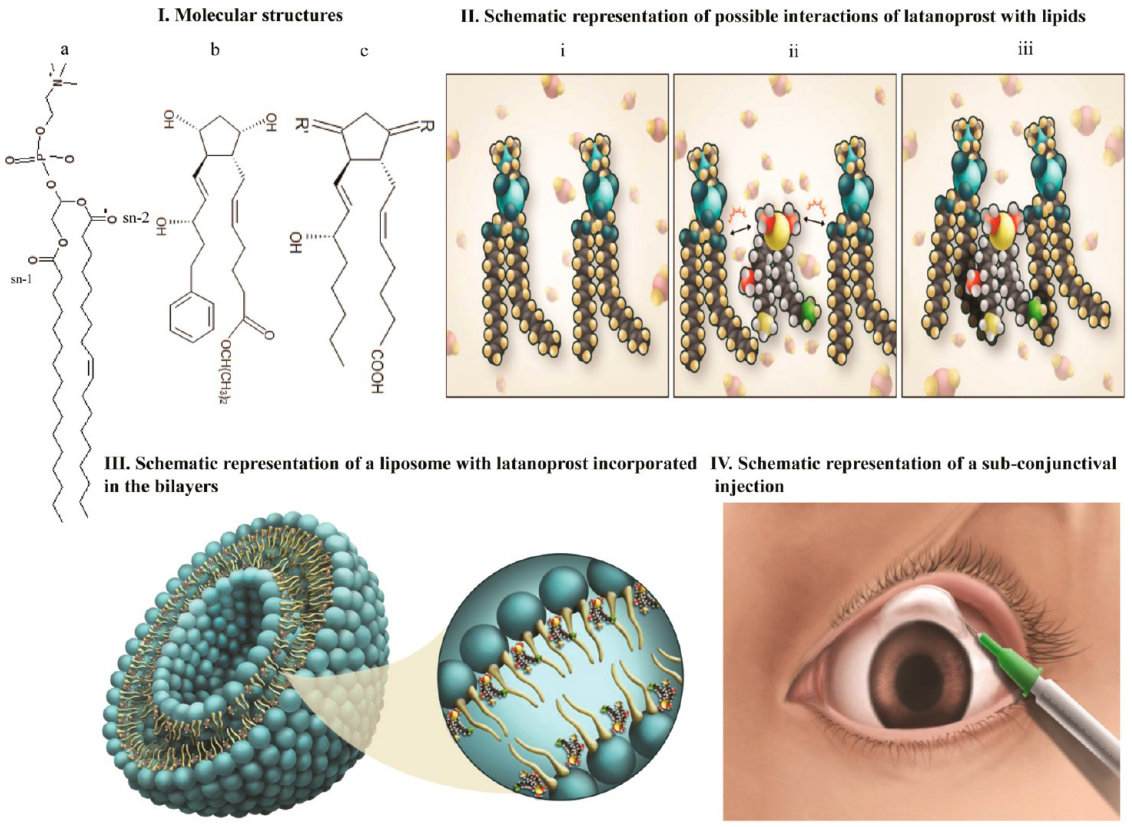

Figure 3. I: Molecular structures. (a) Structure of an EggPC. EggPC is an unsaturated and a naturally derived zwitterionic lipid that has a double bond in one of its lipid backbone. EggPC belongs to the family of glycerophospholipids containing a phosphate group and a choline headgroup. (b) Structure of latanoprost. Latanoprost consists of an isopropyl ester group that is more lipophilic and ready converts into acid by hydrolysis. It also consists of an aromatic ring, which prevents omega-oxidation, and three hydroxyl groups in its backbone. (c) Structure of prostenoic acid. II: General schematic representation of sequential interactions of latanoprost with liposomes. (i) Arrangement of individual phosphocholines (EggPC) with water molecules surrounding polar headgroups before latanoprost titration. (ii) Enthalpic contributions due to hydrogen bond formation between the polar part of latanoprost (OH group) and lipid backbone at the interface. (iii) Entropic contributions due to desolvation of both the polar and nonpolar part of latanoprost, with the hydrophobic domain buried along the lipid acyl chains. III: Schematic representation of a liposome with latanoprost incorporated in the bilayers. IV: Schematic representation of a subconjunctival injection into the patient's eye beneath the upper eyelid. A small bleb is clearly seen where the liposomal formulation has been administered and usually disappears within 30 min.

instructive to examine the drug and lipid structure more closely.

The molecular structures of EggPC, prostenoic acid, and latanoprost are shown in Figure 3I. The predominant structure (C16:0, C18:1) in EggPC is a phosphatidylcholine consisting of a choline headgroup and glycerophosphoric acid connected to two long fatty acyl chains with the presence of an unsaturation in one of the fatty acyl chains (C18:1) (Figure 3Ia). Prostaglandins contain an oxygenated cyclopentane ring with a heptenoic acid side chain and an octenoic side chain arranged on adjacent carbon atoms of the ring. Latanoprost (13,14-dihydro-17-phenyl-18,19,20-trinor-PGF2α-isopropyl ester) is a prostaglandin analogue (PGF2α) where the heptenoic side chain contains an isopropyl ester, which is more lipophilic, and the octenoic side chain consists of an aromatic phenyl ring substituent (Figure 3Ib).[31] The basic structural unit is prostenoic acid (Figure 3Ic).

At binding site 1, a favorable enthalpy change (ΔH_1 −4.4 kcal/mol) was observed, suggesting that the initial binding of latanoprost was mediated by strong hydrogen bonding between the hydroxyl group present in latanoprost and the carbonyl ester group (at sn-1 and/or sn-2 positions) present at the interface between the polar and nonpolar part of the lipid. The enthalpy change obtained (ΔH_1) was similar in magnitude to previously reported values, suggesting strong and unidirectional hydrogen bonding.[30,32,33]

The entropy change ($T\Delta S_1$ +2.4 kcal/mol) was favorable and could be attributed due to an increase in solvent entropy due to exclusion of solvent (buffer) molecules from both polar and nonpolar domains upon latanoprost binding.

An increase in overall Gibbs free energy was observed ($\Delta G_2 > \Delta G_1$) with further addition of the drug to the liposome at binding site 2. A favorable enthalpy change was observed (ΔH_2 −1.7 kcal/mol) but with a lower magnitude at binding site 2. A lower enthalpy (ΔH_2) change suggests the possibility of a weaker van der Waals force[30] and $\pi-\pi$ interactions between the double bonds present in the lipid backbone (C18:1)

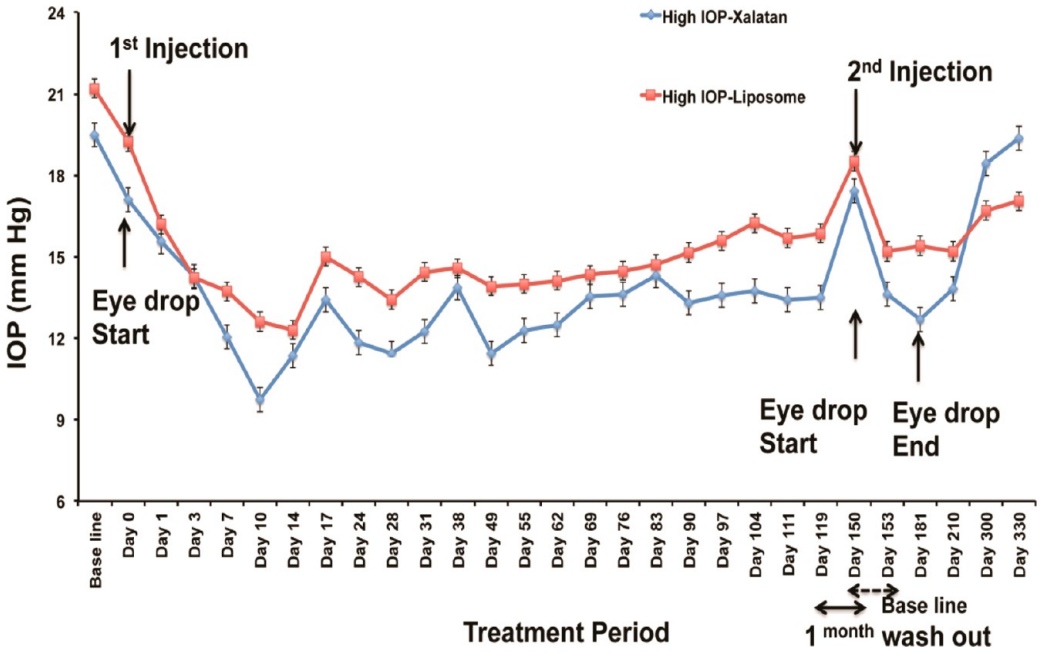

Figure 4. Intraocular pressure measurements. Comparison of intraocular pressure (IOP) measurements between Xalatan (topical eye drops) and latanoprost-loaded EggPC liposomes (subconjunctival injection) in nonhuman primates. A single subconjunctival injection of latanoprost-loaded liposomes led to IOP reduction for up to 120 days and was comparable to daily topical eye drops (Xalatan). Subsequently, a second injection was administered, and the IOP was further reduced over another 180 days.

and in one of the side chains present around the cyclopentane ring of latanoprost. However, the lower enthalpy change (ΔH_2) was accompanied by a greater favorable entropy change ($T\Delta S_2$ +6.7 kcal/mol) due to an increase in solvent entropy caused by further solvent exclusion.

Taking into account the different thermodynamic parameters evaluated by ITC, the binding of latanoprost with EggPC liposomes was found to be driven by favorable enthalpy (hydrogen bonding, weak van der Waals force and $\pi-\pi$ interaction) and favorable entropy changes. These results suggest that the similarity of molecular structures between the lipid (EggPC) and drug (latanoprost) is the dominant factor driving the favorable binding/interaction/partitioning; such favorable interactions, as well as structural similarity in turn, can be used to explain the improved stability, enhanced loading, and the sustained release. A schematic of latanoprost interaction with EggPC liposomes is shown in Figure 3II. A schematic of a liposome with latanoprost incorporated in bilayers is shown in Figure 3III.

On the basis of ITC results, we expect that other prostaglandin analogues such as travoprost, bimatoprost, and unoprostone isopropyl that share similar molecular structures could be developed for sustained delivery using liposomes. This could highlight a unique strategy for the favorable incorporation of prostaglandins with liposomes. Also, to our knowledge, there are no reported studies to evaluate the thermodynamic properties of hydrophobic drugs with liposomes in buffer conditions using ITC.[34−37] This novel method can be a powerful tool to elucidate the molecular interactions of other hydrophobic drugs with liposomes. The insights gained from these studies will assist to identify and select the optimal drug and liposome for sustained delivery applications. This novel method will find its applications in drug discovery and/or drug delivery programs in the future.

Safety and Efficacy in Ocular Hypertensive Nonhuman Primates. To understand how the *in vitro* stability and sustained release translate into an *in vivo* model, we evaluated the safety and efficacy of latanoprost-loaded EggPC liposomes in ocular hypertensive nonhuman primates. The IOP decreased following subconjunctival injection (schematic in Figure 3IV) of latanoprost-loaded EggPC liposomes, and the IOP lowering was comparable to daily Xalatan treatment (up to 120 days) at each measured time point and was not statistically significant between the two groups. The mean IOP was 14.99 mmHg (95% CI 14.6 to 15.4) in group 1 and 15.03 mmHg (95% CI 14.7 to 15.4) in group 2; p = 0.832. The repeated injection showed a significant drop from baseline IOP in group 1 (p = 0.032) and demonstrated the linearly independent pairwise test for each time point (Bonferroni test) (Figure 4). In our study, we compared the efficacy of IOP lowering between subconjunctival injection of latanoprost-loaded EggPC liposomes and topical latanoprost eye drops, without the need for comparison against subconjunctival injection of latanoprost eye drops.

We believe that latanoprost eye drops, if injected subconjunctivally, cannot sustain IOP lowering for more than a few days due to lower loading of latanoprost (50 μg/mL) in Xalatan when compared to a ~20-fold increase in loading concentration (~1 mg/mL) of latanoprost in liposomal nanocarriers. This points to the benefit and importance of payload for maintaining therapeutically relevant concentrations for sustained efficacy over extended periods of time (more than 3 months). Also, a repeat injection resulted in sustained IOP lowering of over 180 days, confirming the reproducibility and tolerability of using a liposomal formulation.

Our previous studies with latanoprost-loaded EggPC liposomes showed IOP lowering up to 90 days in normal IOP rabbit eyes.[15] The observed difference in IOP lowering between monkey and rabbit eyes could be attributed to species difference[38] and the presence or absence of a pigment melanin.[39] The rabbits used in our previous studies were normotensive New Zealand white rabbits and lacked the pigment melanin. Studies reported have shown a direct correlation of latanoprost binding with melanin on IOP lowering.[39] Also, Nomura *et al.* reported the comparison of topical latanoprost on IOP lowering between monkey and rabbit eyes.[38] Their studies concluded that high IOP lowering in monkey eyes was caused by an increased selectivity of latanoprost toward prostaglandin F receptors (FP) as well as the differences in receptor subtype expression levels across different species. The main mechanism of latanoprost on IOP lowering is thought to be mediated by uveoscleral outflow of aqueous humor with structural changes and functional properties of the extracellular matrix components present in ciliary muscle.[38]

There was no evidence of any adverse effect (Supplementary Figure S2) with repeated injections. Latanoprost eye drops have been reported to be a potential causative factor in the development of cystoid macular edema (CME). Nevertheless, a direct relationship between the occurrence of CME in eyes being treated with latanoprost has not been established.[40] For this reason, we examined the retina of the monkey eyes for any evidence of clinically significant CME. The average macular thickness of the retina remained unchanged before and after treatment for all the treatment groups (Supplementary Table S2). These results confirmed that subconjunctival injections of liposomes were indeed a safe drug delivery platform for sustained drug release for glaucoma medical therapy.

Moon *et al.* reported that subconjunctival injection of liposome-bound low-molecular-weight heparin (LMWH) behaved like a depot system with improved absorption of low molecular weight heparin. The released LMWH remained (up to 120 h) at the site of injection due to larger particle size (~550 nm).[41] However, the mechanism of action in our studies could be different due to smaller particle size (~100 nm). Upon subconjunctival injection, the nanosized carriers (with or without latanoprost) may not be localized in the subconjunctival space; dispersal to other regions cannot be ruled out at this point without additional studies.

There could be two possible explanations for longer *in vivo* effect (120 days) when compared to *in vitro* release (~60 days assuming release to total completion). One is that release of latanoprost is slower in the eye, due to the lower volume of liquid in the eye leading to partitioning-limited release; the other possibility is that the released latanoprost is also not cleared fast from the eye. Experiments to verify the proposed mechanisms are currently in progress. Nevertheless, it should be clear that we have developed a sustained-release nanomedicine product that is safe and effective. This product is currently under investigation for safety and efficacy in phase I human trials in Singapore.

CONCLUSIONS

In conclusion, we have developed a nanocarrier with the capability of sustained release for ocular indications. Specifically, the developed nanocarrier demonstrated sustained efficacy (IOP lowering up to 120 days with a single subconjunctival injection) and proved to be well tolerated in a diseased nonhuman primate model, making it a prime sustained-release nanomedicine candidate for glaucoma therapy. The reasons for both the sustained release and the stability of the latanoprost-loaded liposomes have been elucidated with binding studies and partitioning arguments. Similar concepts may be used to develop other suitable nanocarriers for sustained release.

MATERIALS AND METHODS

Egg phosphatidylcholine (EggPC > 95 wt %) was purchased from NOF Corporation, Japan. Latanoprost was purchased from Chemical Testing and Calibration Laboratories, China. Polycarbonate filter membrane of size 0.08 μm and drain discs were purchased from Northern Lipids Inc., Canada. Cellulose ester dialysis bags (10 mm dia × 16 mm flat width) were purchased from Spectrum Laboratories, USA. Sodium phosphate dibasic anhydrous (Na_2HPO_4), potassium phosphate monobasic anhydrous (KH_2PO_4), potassium chloride (KCl), and sodium chloride (NaCl) salts were purchased from Sigma, USA, and used without further purification. The water used in all the experiments was from a MiliQ purification system with a resistivity of at least 18.2 ± 0.2 mΩ cm. All solvents for drug estimation were of high-performance liquid chromatography (HPLC) grade (>99% purity) and were purchased from Tedia, USA.

Light Scattering Studies. *a. Dynamic Light Scattering (Determination of Hydrodynamic Radius (R_h) and Translational Diffusion Coefficient (D_t)).* The average hydrodynamic radius

(R_h) and translational diffusion coefficient (D_t) of liposomes were measured using a Brookhaven laser light scattering system. The instrument consists of a BI200SM goniometer (Ver. 2.0), BI-900AT digital correlator, and data acquisition software with accessories. The laser source was a helium−neon diode laser with a wavelength of 636 nm. The entire instrumental setup was connected to a digitally controlled water bath. The laser power and/or the pinhole size were adjusted to achieve a targeted count rate for a good signal-to-noise ratio ranging between 200 and 500 kcps (kilocounts per second). The laser source was stabilized for half an hour prior to measurements, and subsequent data acquisitions were collected. A pinhole size of 0.4 μm with a laser power of 5−15 mW was used to achieve a good signal-to-noise ratio. To reduce any interference due to beam refractions from scratches and bubbles in the sample glass tubes, the filling liquid (decahydronapthalene) in the sample port was recirculated and filtered through a 0.2 μm filter for 15 min. The hydrodynamic radius of the liposomes (R_h) was measured from the data analyzed by the GENDIST program from the conversion of decay rate distribution by inverse Laplace transformation. The probability of reject was set to 0.5.

The buffer, PBS pH 5.5, was prefiltered using a 0.45 μm cellulose ester syringe filter to remove any dust particles. Plain EggPC liposomes and latanoprost-loaded EggPC liposomes were diluted with filtered PBS pH 5.5 to a final concentration range of 0.09−0.18 mM. The samples were measured at different scattering angles ranging between 55° and 135° and at two different temperatures, 25 and 37 °C. A plot of Γ (decay rate) *vs* q^2 (square of the scattering vector) for spherical particles was known to be angle dependent. The slope of the data points from a linear fit will result in the value of the translational diffusion coefficient (D_t), and hydrodynamic radius (R_h) was calculated from Stokes−Einstein equation as shown in eq 1:

$$R_h = \frac{k_b T}{6\pi\eta D_t} \quad (1)$$

where R_h = hydrodynamic radius (m), k_b = Boltzmann constant (J/K = kg·m^2/s^2·K), T = temperature (K), η = solvent viscosity (kg/m·s), and D_t = translational diffusion coefficient (m^2/s).

b. Static Light Scattering (Estimation of Radius of Gyration (R_g) and Shape Factor (S)). Static light scattering is based on the principle of time-averaged intensities of the scattered light and yields information on the structural properties, such as size and shape of the particles. Different physical parameters such as radius of gyration (R_g) and shape factor (S) were determined from static light scattering techniques. R_g was determined by partial Berry plot. Plain EggPC and latanoprost-loaded EggPC liposomes were diluted with filtered PBS pH 5.5. The final concentration of liposomes was 0.09 mM and was measured at 25 and 37 °C. The pinhole size was set to 1 mm. The laser power was adjusted between 5 and 15 mW such that the scattered intensity was within 1000 kcps. Measurements were carried out over 10 different angles ranging from 55° to 135° with 10° increments.

The equation for the partial Berry plot is shown in eq 2:

$$(1/I(q))^{1/2} = C(1 + R_g{}^2 q^2/6) \quad (2)$$

where $I(q)$ = intensity of scattered light, R_g = hydrodynamic radius (m), q = scattering wave vector, and its magnitude is given in eq 3:

$$q = \frac{4\pi n}{\lambda} \sin(\theta/2) \quad (3)$$

where n = refractive index of the liquid, λ = wavelength of light source in a vacuum, R_g was determined from the slope and the intercept of $(1/I(q))^{1/2}$ *vs* q^2, and the shape factor (S) was determined using principles of both static and dynamic light scattering. The value for S is given by eq 4:

$$S = R_g/R_h \quad (4)$$

Cryo-transmission Electron Microscopy (cryo-TEM). The cryo-TEM studies were performed with a Carl Zeiss Libra 120 Plus transmission electron microscope (Germany). The instrument was operated at 120 kV in zero-loss bright field mode. Digital images were recorded under low-dose conditions using a TRS Sharp Eye slow-scan dual-speed CCD camera (Troendle, Moorenwies, Germany) controlled by the ITEM software (Olympus-SIS, Soft Image System, Munster, Germany). Plain EggPC and latanoprost-loaded EggPC liposomes (initial drug/lipid wt ratio of 0.1) were prepared using passive loading and an extrusion technique similar to the method outlined previously.[15] A 1−2 μL amount of plain EggPC and latanoprost-loaded EggPC liposomes was deposited on the lacey Formvar grid that was treated with 30 s of glow discharge using a JEOL HDT-400 hydrophilic treatment device under controlled room temperature (25 °C) and humidity. Any excess sample was blotted for 3 s using a filter paper in a Gatan Cryoplunge 3 (Cp3). The samples were quickly vitrified inside liquid ethane and immediately transferred to liquid nitrogen to minimize sample deformations and/or ice crystal formation during transfer.

Isothermal Titration Calorimetry. A microcalorimeter is widely used to determine the reaction thermodynamics and binding energetics. The binding of latanoprost with EggPC liposomal nanocarriers was studied using a MicroCal instrument (MicroCal, USA). This instrument works on the principle of power compensation between two cells (sample and reference cell) caused by the differences in the heat released or absorbed upon binding of the drug with liposomes. The measurements were conducted under isothermal conditions (at 37 °C), and any temperature fluctuations were suppressed by heat compensation at sink to minimize error. The instrument consists of a reference and a sample cell that holds a sample volume of 1.45 mL, while the syringe buret holds a volume of 282 μL. The titrations were carried out with sequential injections of the samples from the syringe buret into the sample cell with continuous mixing. The tip of the syringe acts like a blade-type stirrer to ensure uniform stirring during the course of the titration. Different injection parameters can be controlled with the online software interface provided by the supplier. Absolute care was taken to ensure matching background buffer in the cells or else heat changes caused due to this mismatch will lead to erroneous results.

A method suitable to study the interaction of a hydrophobic drug, latanoprost, with liposomes was considered more challenging due to the limited solubility of the drug in buffer (~50 μg/mL). Most of the studies have reported the binding of hydrophilic drugs to liposomes due to the advantage of higher solubility in aqueous-based buffer systems.[36,42] To our knowledge, there are no methods reported to study the interaction of a hydrophobic drug with liposomes. In this work, we developed a novel experimental protocol of using a solvent mixture (40% DMSO/60% PBS, pH 5.5) to study latanoprost binding with liposomes. Latanoprost was dissolved in the solvent mixture (2.54 mM) loaded into a syringe (0.282 mL) and titrated against plain EggPC liposomes (10.8 mM) diluted in the same solvent mixture placed in the sample cell (1.45 mL). The titrations were carried out at 37 °C. A sequential binding model with two sites available for latanoprost binding into liposomes was used to fit the integrated enthalpy data after background subtraction (heat of dilution) from the software provided by Microcal. The equation for a sequential binding model[43] with two sites is given by eq 5:

$$Q_i{}^{tot} = V_0 E_{tot}[(\Delta H_1 K_1 P) + (\Delta H_1 + \Delta H_2) K_1 K_2 P^2]/(1 + K_1 P + K_1 K_2 P^2) \quad (5)$$

where $Q_i{}^{tot}$ = total heat after the ith injection, V_o = volume of the calorimetric cell, K_1 and K_2 are observed equilibrium binding affinities at each site, ΔH_1 and ΔH_2 are the corresponding enthalpy changes, P = free drug concentration, and E_{tot} = total liposome concentration. K_1 and K_2 were estimated by fitting the experimental data to the two-site sequential binding model[43] with data analysis evaluated by the software provided by Microcal. Values for the change in free energy (ΔG) were calculated using the relation $(\Delta G) = -RT \ln(K)$, where R is the gas constant (1.9872 cal K^{-1} mol^{-1}) and T the absolute temperature.

The run parameters included were (i) no. of injections, 51, (ii) temperature, 37 °C, (iii) stirring speed, 307, (iv) feedback mode, high, (v) ITC equilibration options, fast and auto,

(vi) injection volumes (a) 10 injections, 1 μL; (b) 10 injections, 2 μL; (c) 10 injections, 4 μL; (d) 21 injections, 10 μL; (e) duration, 4 s; (f) spacing, 150 s; (g) filter period, 2 s; and (h) scans, identical.

Animal Preparation and Anesthesia. Experimentation on nonhuman primates (*Macaca fascicularis*) that exhibit ocular hypertension as defined as an IOP > 18 mmHg, was performed in accordance with the statement for the use of animals in ophthalmic and vision research approved by the Association for Research in Vision and Ophthalmology. The guidelines of the Animal Ethics Committee of the Singhealth Singapore Association for Assessment and Accreditation of Laboratory Animal Care were also satisfied. Nonhuman primates were anesthetized by intramuscular injection of a mixture containing ketamine (5−10 mg/kg body weight) and acepromazine maleate (0.25 mg/kg body weight) and subcutaneous injection of atropine sulfate (0.125 mg/kg body weight). Their airway, respiration, and pulse were monitored during all procedures. One to two drops of 1% xylocaine was used as topical anesthesia to reduce possible discomfort to the animals involved during the procedure. Pupils of nonhuman primates were dilated with 2.5% phenylephrine hydrochloride and 1% tropicamide drops (Alcon Laboratories, Frenchs Forest, NSW, Australia).

Treatment Groups. Seven nonhuman primates were used in this study and were divided into two groups. Group 1: received a single 100 μL subconjunctival injection of latanoprost-loaded EggPC liposomes[15] into both eyes (n = 4). Group 2: received once daily latanoprost (Xalatan, 50 μg/mL) eyedrops into both eyes (n = 3). The animals were followed up until the IOP in group 1 returned to baseline IOP. This signaled the end of therapeutic efficacy and duration of hypotensive effect of the liposome formulation. A cessation of daily eye drop administration for group 2 with a 1 month washout allowed the IOP to return to baseline. For group 1, a repeat subconjunctival injection of latanoprost-loaded EggPC liposomes was then performed.

Subconjunctival Injection in Nonhuman Primates. Group 1 received 100 μL of latanoprost-loaded EggPC liposomes injected subconjunctivally using a 30-gauge needle under aseptic conditions. The formulation was injected in a controlled manner into the superior bulbar conjunctiva as described previously.[15]

Intraocular Pressure Measurements. The monkeys were slightly anesthetized with ketamine (5 mg/kg body weight) for measurements of IOP. One to two drops of 1% xylocaine was used as topical anesthesia to reduce possible discomfort to the animals involved during the measurement procedure. IOP was measured using a calibrated tonometer (Tono-Pen XL, Reichert Technologies, Depew, NY, USA). The schedule for IOP measurements was as follows: IOP measured at 2−4 pm every day for 1 month and then weekly for the next 3 months followed by measurements thereafter every month until IOP returned to baseline IOP. A once daily baseline IOP measurement to both eyes of all animals was recorded prior to commencement of the treatment consecutively for 3 days. A mean IOP was taken from six consecutive IOP measurements at each time point. The treatment was commenced on day 4 for all the animals.

Statistical Analysis. Comparisons at each time point between control and test groups were conducted using Mann−Whitney U test. In addition, Wilcoxon signed ranks tests were conducted to test between eye comparisons. Within group comparisons were also conducted using Wilcoxon signed rank tests. A linear mixed model analysis was conducted to adjust for the correlated repeated IOP measures taken during the trial and compared the control and test groups as well as to adjust for the other eye. Hurvich and Tsai's criterion (AICC) was used for the small sample size consideration for model fitting, and results are from applying compound symmetry variance−covariance/correlation structure, which showed the lowest AICC value of 320.7 compared to diagonal (339.6) and unstructured (341.4) variance−covariance/correlation structures. Significance was set at 0.05 levels. SPSS version 19 (IBM SPSS Statistics, Chicago, IL, USA) was used for all analyses.

Conflict of Interest: The authors declare the following competing financial interest(s): S. S. Venkatraman and T. T. Wong are directors of Peregrine Ophthalmic Pte. Ltd. (herein known as entity). Collectively with F. Boey and J. V. Natarajan, they are also shareholders of the entity. Peregrine Ophthalmic Pte. Ltd. has no approved products at this time, but is involved in the development of sustained delivery of ophthalmic agents for various ocular diseases. The lead product LipoLat (liposomal latanoprost) is currently being evaluated in clinical trials. Peregrine Ophthalmic Pte. Ltd. has licensed technology co-developed by S. S. Venkatraman, T. T. Wong, F. Boey, and J. V. Natarajan, with patent pending for approval.

Acknowledgment. The authors would like to acknowledge the financial support provided by the National Research Foundation−Funded Translational and Clinical Research (TCR) Programme Grant [NMRC/TCR/002−SERI/2008−TCR 621/41/2008]. J.V.N. would like to acknowledge the funding from the Canadian Commonwealth Scholarship Program (CCSP) to pursue research at University of Waterloo as a visiting scholar for six months. The authors would like to thank H. Fan (Department of Chemical Engineering, University of Waterloo) for help with the training on light scattering instrument and isothermal titration calorimeter. The authors would like to thank T. Y. Yan (FACTS Lab, School of Materials Science and Engineering, Nanyang Technological University) for help with Cryo-TEM.

Supporting Information Available: This material is available free of charge via the Internet at http://pubs.acs.org.

REFERENCES AND NOTES

1. Farokhzad, O. C.; Langer, R. Impact of Nanotechnology on Drug Delivery. *ACS Nano* **2009**, *3*, 16–20.
2. Duncan, R.; Gaspar, R. Nanomedicine(s) under the Microscope. *Mol. Pharmaceutics* **2011**, *8*, 2101–2141.
3. Wagner, V.; Dullaart, A.; Bock, A. K.; Zweck, A. The Emerging Nanomedicine Landscape. *Nat. Biotechnol.* **2006**, *24*, 1211–1217.
4. Vasir, J. K.; Labhasetwar, V. Biodegradable Nanoparticles for Cytosolic Delivery of Therapeutics. *Adv. Drug Delivery Rev.* **2007**, *59*, 718–728.
5. Allen, T. M.; Cullis, P. R. Liposomal Drug Delivery Systems: From Concept to Clinical Applications. *Adv. Drug Delivery Rev.* **2013**, *65*, 36–48.
6. Torchilin, V. P. Micellar Nanocarriers: Pharmaceutical Perspectives. *Pharm. Res.* **2007**, *24*, 1–16.
7. Maeda, H.; Bharate, G. Y.; Daruwalla, J. Polymeric Drugs for Efficient Tumor-Targeted Drug Delivery Based on EPR-Effect. *Eur. J. Pharm. Biopharm.* **2009**, *71*, 409–419.
8. Haran, G.; Cohen, R.; Bar, L. K.; Barenholz, Y. Transmembrane Ammonium-Sulfate Gradients in Liposomes Produce Efficient and Stable Entrapment of Amphiphatic Weak Bases. *Biochim. Biophys. Acta, Biomembr.* **1993**, *1151*, 201–215.
9. Chang, H. I.; Yeh, M. K. Clinical Development of Liposome-Based Drugs: Formulation, Characterization, and Therapeutic Efficacy. *Int. J. Nanomed.* **2012**, *7*, 49–60.
10. Quigley, H. A.; Broman, A. T. The Number of People with Glaucoma Worldwide in 2010 and 2020. *Br. J. Ophthalmol.* **2006**, *90*, 262–267.
11. Gooch, N.; Molokhia, S. A.; Condie, R.; Burr, R. M.; Archer, B.; Ambati, B. K.; Wirostko, B. Ocular Drug Delivery for Glaucoma Management. *Pharmaceutics* **2012**, *4*, 197–211.
12. Maurice, D.; Mishima, S. Ocular Pharmacokinectis. In *Handbook of Experimental Pharmacology*; Sears, M. L., Ed.; Springer: Berlin, Germany, 1984; pp 16−119.
13. Tsai, T.; Robin, A. L.; Smith, J. P., 3rd. An Evaluation of How Glaucoma Patients Use Topical Medications: A Pilot Study. *Trans. Am. Ophthalmol. Soc.* **2007**, *105*, 29–33.
14. Nordstrom, B. L.; Friedman, D. S.; Mozaffari, E.; Quigley, H. A.; Walker, A. M. Persistence and Adherence with Topical Glaucoma Therapy. *Am. J. Ophthalmol.* **2005**, *140*, 598–606.
15. Natarajan, J. V.; Ang, M.; Darwitan, A.; Chattopadhyay, S.; Wong, T. T.; Venkatraman, S. S. Nanomedicine for Glaucoma: Liposomes Provide Sustained Release of Latanoprost in the Eye. *Int. J. Nanomed.* **2012**, 7.
16. Barenholz, Y. Doxil®—The First FDA-Approved Nano-Drug: Lessons Learned. *J. Controlled Release* **2012**, *160*, 117–134.

17. Atyabi, F.; Farkhondehfai, A.; Esmaeili, F.; Dinarvand, R. Preparation of Pegylated Nano-Liposomal Formulation Containing SN-38: *In Vitro* Characterization and *in Vivo* Biodistribution in Mice. *Acta Pharm.* **2009**, *59*, 133–144.
18. Bhardwaj, U.; Burgess, D. J. Physicochemical Properties of Extruded and Non-Extruded Liposomes Containing the Hydrophobic Drug Dexamethasone. *Int. J. Pharm.* **2010**, *388*, 181–189.
19. Kim, C. K.; Park, D. K. Stability and Drug Release Properties of Liposomes Containing Cytarabine as a Drug Carrier. *Arch. Pharmacal Res.* **1987**, *10*, 75–79.
20. Drummond, D. C.; Meyer, O.; Hong, K. L.; Kirpotin, D. B.; Papahadjopoulos, D. Optimizing Liposomes for Delivery of Chemotherapeutic Agents to Solid Tumors. *Pharmacol. Rev.* **1999**, *51*, 691–743.
21. Charrois, G. J. R.; Allen, T. M. Drug Release Rate Influences the Pharmacokinetics, Biodistribution, Therapeutic Activity, and Toxicity of Pegylated Liposomal Doxorubicin Formulations in Murine Breast Cancer. *Biochim. Biophys. Acta, Biomembr.* **2004**, *1663*, 167–177.
22. Johnston, M. J.; Edwards, K.; Karlsson, G.; Cullis, P. R. Influence of Drug-to-Lipid Ratio on Drug Release Properties and Liposome Integrity in Liposomal Doxorubicin Formulations. *J. Liposome Res.* **2008**, *18*, 145–157.
23. Johnston, M. J.; Semple, S. C.; Klimuk, S. K.; Edwards, K.; Eisenhardt, M. L.; Leng, E. C.; Karlsson, G.; Yanko, D.; Cullis, P. R. Therapeutically Optimized Rates of Drug Release Can be Achieved by Varying the Drug-to-Lipid Ratio in Liposomal Vincristine Formulations. *Biochim. Biophys. Acta, Biomembr.* **2006**, *1758*, 55–64.
24. Zhigaltsev, I. V.; Maurer, N.; Akhong, Q. F.; Leone, R.; Leng, E.; Wang, J.; Semple, S. C.; Cullis, P. R. Liposome-Encapsulated Vincristine, Vinblastine and Vinorelbine: A Comparative Study of Drug Loading and Retention. *J. Controlled Release* **2005**, *104*, 103–111.
25. Liu, J. B.; Lee, H.; Huesca, M.; Young, A. P.; Allen, C. Liposome Formulation of a Novel Hydrophobic Aryl-Imidazole Compound for Anti-Cancer Therapy. *Cancer Chemother. Pharmacol.* **2006**, *58*, 306–318.
26. Pandelidou, M.; Dimas, K.; Georgopoulos, A.; Hatziantoniou, S.; Demetzos, C. Preparation and Characterization of Lyophilised Egg PC Liposomes Incorporating Curcumin and Evaluation of Its Activity Against Colorectal Cancer Cell Lines. *J. Nanosci. Nanotechnol.* **2011**, *11*, 1259–1266.
27. Kan, P.; Tsao, C. W.; Wang, A. J.; Su, W. C.; Liang, H. F. A Liposomal Formulation Able to Incorporate a High Content of Paclitaxel and Exert Promising Anticancer Effect. *J. Drug Delivery* **2011**, *2011*, 629234.
28. Khan, D. R.; Rezler, E. M.; Lauer-Fields, J.; Fields, G. B. Effects of Drug Hydrophobicity on Liposomal Stability. *Chem. Biol. Drug Des.* **2008**, *71*, 3–7.
29. Bernsdorff, C.; Reszka, R.; Winter, R. Interaction of the Anticancer Agent Taxol (TM) (paclitaxel) with Phospholipid Bilayers. *J. Biomed. Mater. Res.* **1999**, *46*, 141–149.
30. Kawasaki, Y.; Freire, E. Finding a Better Path to Drug Selectivity. *Drug Discovery Today* **2011**, *16*, 985–990.
31. DeRuiter, J. Prostaglandins and the Eicosanoids. *Principles Drug Action* **2002**, 1–28.
32. Kawasaki, Y.; Chufan, E. E.; Lafont, V.; Hidaka, K.; Kiso, Y.; Mario Amzel, L.; Freire, E. How Much Binding Affinity Can Be Gained by Filling a Cavity? *Chem. Biol. Drug Des.* **2010**, *75*, 143–151.
33. Lafont, V.; Armstrong, A. A.; Ohtaka, H.; Kiso, Y.; Mario Amzel, L.; Freire, E. Compensating Enthalpic and Entropic Changes Hinder Binding Affinity Optimization. *Chem. Biol. Drug Des.* **2007**, *69*, 413–422.
34. Wu, G. H.; Lee, K. Y. C. Interaction of Poloxamers with Liposomes: An Isothermal Titration Calorimetry Study. *J. Phys. Chem. B* **2009**, *113*, 15522–15531.
35. Trandum, C.; Westh, P.; Jorgensen, K.; Mouritsen, O. G. Association of Ethanol with Lipid Membranes Containing Cholesterol, Sphingomyelin and Ganglioside: a Titration Calorimetry Study. *Biochim. Biophys. Acta, Biomembr.* **1999**, *1420*, 179–188.
36. Ikonen, M.; Murtomaki, L.; Kontturi, K. Microcalorimetric and Zeta Potential Study on Binding of Drugs on Liposomes. *Colloids Surf., B* **2010**, *78*, 275–282.
37. Manrique-Moreno, M.; Howe, J.; Suwalsky, M.; Garidel, P.; Brandenburg, K. Physicochemical Interaction Study of Non-Steroidal Anti-Inflammatory Drugs with Dimyristoylphosphatidylethanolamine Liposomes. *Lett. Drug Des. Discovery* **2010**, *7*, 50–56.
38. Nomura, S.; Hashimoto, M. Pharmacological Profiles of Latanoprost (Xalatan), a Novel Anti-Glaucoma Drug. *Nihon Yakurigaku Zasshi.* **2000**, *115*, 280–286.
39. Stjernschantz, J. W. From PGF(2 alpha)-Isopropyl Ester to Latanoprost: A Review of the Development of Xalatan - The Proctor Lecture. *Invest. Ophthalmol. Visual Sci.* **2001**, *42*, 1134–1145.
40. Schumer, R. A.; Camras, C. B.; Mandahl, A. K. Latanoprost and Cystoid Macular Edema: Is There a Causal Relation? *Curr. Opin. Ophthalmol.* **2000**, *11*, 94–100.
41. Moon, J. W.; Song, Y. K.; Jee, J. P.; Kim, C. K.; Choung, H. K.; Hwang, J. M. Effect of Subconjunctivally Injected, Liposome-Bound, Low-Molecular-Weight Heparin on the Absorption Rate of Subconjunctival Hemorrhage in Rabbits. *Invest. Ophthalmol. Visual Sci.* **2006**, *47*, 3968–3974.
42. Seelig, J. Thermodynamics of Lipid-Peptide Interactions. *Biochim. Biophys. Acta, Biomembr.* **2004**, *1666*, 40–50.
43. Kumaran, S.; Jez, J. M. Thermodynamics of the Interaction between O-Acetylserine Sulfhydrylase and the C-Terminus of Serine Acetyltransferase. *Biochemistry* **2007**, *46*, 5586–5594.